

# Modelling the Long-Term and Inter-Annual Variability in the Laptev Sea Hydrography and Subsea Permafrost State

by Elena Golubeva<sup>1,2</sup>, Gennady Platov<sup>1,2</sup>, Valentina Malakhova<sup>1</sup>,  
Marina Kraineva<sup>1</sup> and Dina Iakshina<sup>1,2</sup>

**Abstract:** The focus of the presented study is the variability of the hydrology of the Laptev Sea. The study analyses results from three-dimensional coupled ice-ocean regional models of different horizontal resolutions. The Laptev Sea circulation and its inter-annual variability are simulated on the basis of a large-scale model of the Arctic and North Atlantic. The second model is a nested ocean model focused on the Lena River Delta surroundings with an enhanced grid resolution. Both models are forced by the NCEP/NCAR Reanalysis.

The simulated high variability of summer circulation over the Laptev shelf is mainly caused by the difference in the local prevailing wind patterns. The analysis of the Lena river model tracer pathways shows that in summer, the pronounced offshore or onshore transport occurs in certain years, while generally, the circulation pattern is much more complicated being subject to wind forcing, position of the ice edge, and intensity of the river runoff. When the cyclonic circulation of the atmosphere is predominant, the heat and fresh water anomalies, formed due to the sea surface fluxes and the river runoff, penetrate down to the bottom layers.

The model results suggest that the response of winter hydrography to the variability of atmospheric circulation is less pronounced. The salinity pattern, formed during the autumn period under the influence of the wind, persists for a long period during winter and gradually changes under the influence of sea-ice formation processes and on contact with the adjacent water areas. Our simulations show that there was a possibility of a pronounced increase in the near-bottom temperature in the Laptev Sea shelf. The heat flux of the Lena River plays a significant role in this process. The warming of near-bottom waters on the Laptev Sea shelf deserves special attention due to its potential impact on the submarine permafrost, formed during the last glacial cycle, when the Arctic shelf was above sea level. We have performed numerical simulations of the subsea permafrost evolution and the present-day state on the East Siberian Arctic Shelf, using near-bottom temperature provided by the ice-ocean model. Our simulation estimates that the thickness of the permafrost within most of the shelf is 180-550 m, given the geothermal flux value of 60 mW m<sup>-2</sup>. These results show the permafrost upper boundary deepening by ~0.5-5 m from 1948 to 2014 ( $\leq 7.5$  cm yr<sup>-1</sup>) in the shelf. The degradation rate from above is the most rapid in the near-shore coastal zone of the shelf and in the areas affected by the Lena River outflow. Based on the simulations performed, we state that the current warming is not able to destabilize undersea permafrost on the shelf of the Laptev Sea.

**Zusammenfassung:** Im Mittelpunkt der vorliegenden Arbeit steht die hydrologische Variabilität der Laptevsee; sie enthält die Ergebnisse dreidimensionaler, gekoppelter Eis-Ozean-Modelle unterschiedlicher horizontaler Auflösung. Die Zirkulation der Laptevsee und ihre interannuelle Variabilität wird auf der Basis eines großskaligen Modells der Arktis und des Nordatlantiks simuliert. Das zweite Modell ist ein geschichtetes Ozeanmodell unterschiedlicher Auflösung fokussiert auf die Umgebung des Lenadeltas mit erhöhter Netzauflösung. Beide Modelle sind NCEP/NCAR Reanalysis unterstützt. Die simulierte hohe Variabilität der Sommerzirkulation über dem Laptevseeschelf wird hauptsächlich durch Unterschiede im lokal vorherrschenden Windmuster verursacht. Das Flussmodell der Lena zeigt, dass der betonte auf- und ablandige Transport im Sommer in bestimmten Jahren auftritt, während allgemein das Zirkulations-

muster viel komplizierter ist und von der Windstärke, der Lage des Eisrandes und dem Eintrag von Flusswasser abhängt. Bei vorherrschender Tiefdruckzirkulation reichen Wärme- und Süßwasseranomalien bis zum Meeresboden.

Die Modellergebnisse zeigen, dass die Hydrographie im Winter weniger deutlich auf atmosphärische Schwankungen reagiert. Das während des Herbstes unter Windeinfluss gebildete Salinitätsmuster verbleibt für lange Zeit im Winter und verändert sich nur langsam unter dem Einfluss der Meereisbildung und im Kontakt mit den umgebenden Gewässern. Unsere Simulationen zeigen, dass es einen Temperaturanstieg des bodennahen Wassers auf dem Schelf der Laptevsee gibt. Der Wärmeeintrag durch die Lena spielt bei diesem Prozess eine bedeutende Rolle. Die Erwärmung des bodennahen Wassers auf dem Schelf der Laptevsee bedarf besonderer Beachtung wegen eines eventuellen Einflusses auf den submarinen Permafrost, der sich im letzten Glazial ausgebildet hat als der arktische Schelf über dem Meeresspiegel lag. Wir haben numerische Modelle zum submarinen Permafrost und der heutigen Situation des ostsibirischen arktischen Schelfs unter Berücksichtigung der bodennahen Temperaturen aus dem Eis-Ozean-Modell durchgeführt. Unsere Simulation schätzt die Mächtigkeit des Permafrosts auf 180-550 m bei einem geothermischen Wärmefluss von 60 mW m<sup>-2</sup>. Diese Werte zeigen eine Veränderung der Obergrenze des Permafrosts auf dem Schelf von ~0.5-5 m von 1948 bis 2014 ( $\leq 7.5$  cm yr<sup>-1</sup>). Diese Abnahme ist am schnellsten im strandnahen Küstenbereich und dem vom Abfluss der Lena beeinflussten Gebiet. Auf der Basis der durchgeführten Simulationen stellen wir fest, dass die derzeitige Erwärmung nicht ausreicht, den submarinen Permafrost unter dem Schelf der Laptevsee zu destabilisieren.

## INTRODUCTION

The Laptev Sea (Fig. 1), one of the vast Arctic shelf seas, has been the focus of international expeditions over the past decades since TRANSDRIFT I (KASSENS & KARPIY 1994) for several reasons. In summer, the Laptev Sea receives large volumes of fresh water from the Lena River, the annual average discharge is about 540 km<sup>3</sup>/a (SHIKLOMANOV & LAMMERS 2014), which defines a local stratification of the region and supplies heat into the shelf waters (WHITEFIELD et al. 2015). In winter, this region is considered as one of the major “ice factories” in the Arctic, producing a significant amount of sea ice, exported to the Arctic Ocean (ZAKHAROV 1966). The importance of the shelf processes for the Arctic Ocean state is mainly related to the summer export of river freshwater and transport of brine-enriched water, which is formed within the Laptev Shelf in winter due to the permanent sea-ice production (DOBROVOLSKII & ZALOGIN 1982). The riverine export into the central Arctic basin maintains the unique structure of the Arctic halocline, insulating sea-ice from the warmer underlying layer of Atlantic waters, and preventing the sea-ice decline (AAGAARD et al. 1981, STEELE & BOYD 1998).

In recent years a strong hydrographic variability has been observed in the region. A dramatic warming of near-bottom waters (by 2.1 °C in the period from 1984 to 2009) over the Laptev Sea coastal zone was recorded in summer hydro-

**Keywords:** Arctic Ocean, river runoff, freshwater transport, climate variability, subsea permafrost, numerical modelling

doi:10.2312/polarforschung.87.2.195

<sup>1</sup> Institute of Computational Mathematics and Mathematical Geophysics, Siberian Branch Russian Academy of Sciences, Novosibirsk 630090, Russia; <e.golubeva.nsk@gmail.com>

<sup>2</sup> Novosibirsk State University, Novosibirsk, 630090, Russia.

Manuscript received 09 June 2017; accepted in revised form 15 March 2018.

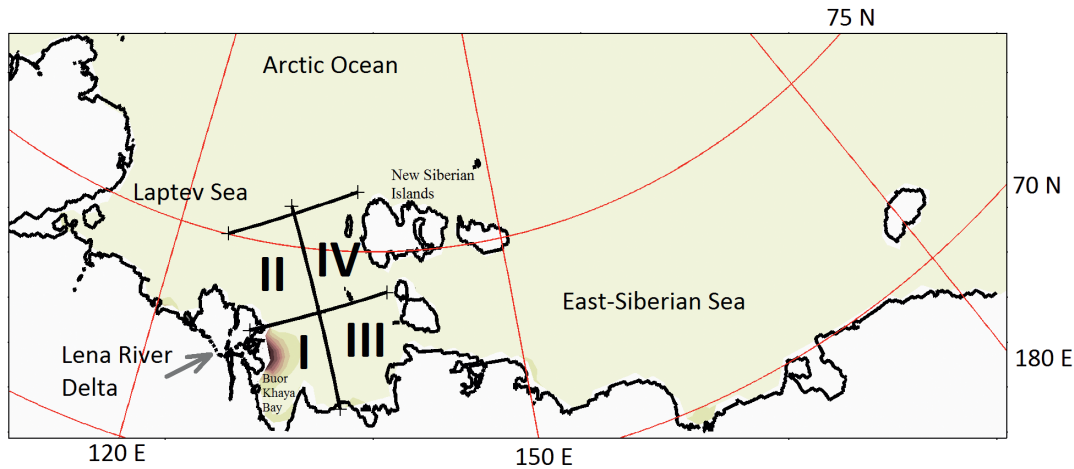


**Fig. 1:** East Siberian Arctic Shelf (ESAS). The region of interest of this study – the eastern Laptev Sea – is divided into four subregions (I – IV).

**Abb. 1:** Übersicht über den Ost-sibirischen Schelf. Das Untersuchungsgebiet im östlichen Laptewmeer ist in vier Subregionen (I – IV) unterteilt.

graphic data for 1920–2009 (DMITRENKO et al. 2011). Several events of unprecedented warming in near-bottom waters, which were believed to be in a near-frozen state all year round, were observed in the central shelf in winter (HÖLEMANN et al. 2011, JANOUT et al. 2013, 2016). These events gave rise to the discussion of a possible impact of this warming on the Laptev Shelf environment.

Large parts of the region are thought to be underlain by submarine permafrost as a result of their exposure during the Last Glacial Maximum, when the global sea levels fell by over one hundred meters (ROMANOVSKII et al. 2005). The state of the permafrost in the Arctic is key to understanding whether methane, a potent greenhouse gas stored in the permafrost-related gas hydrate, can escape to the atmosphere. The dissolved methane concentrations in the waters of the East Siberian Arctic Shelf (ESAS) during the summers from 2003 to 2013 show a widespread supersaturation over large spatial scales (SHAKHOVA et al. 2010, 2014). The ocean bottom water temperature is a significant factor affecting the subsea permafrost distribution (KASSENS et al. 2007, OVERDUIN et al. 2007).

Realizing the potential importance of the region, considerable attention should be paid to the assessment of its present state and identification the physical processes responsible for its variability. The mechanisms responsible for the freshwater modification over the shelves and the water mass exchange between the shelf region and the central Arctic basin are constantly being investigated. Many researchers, based on observations, emphasized the considerable inter-annual variability in summer surface salinity and the river water pathways, correlated with atmospheric circulation (SHPAIKHER et al. 1972, WEINGARTNER et al. 1999, GUAY et al. 2001, DMITRENKO et al. 2005, 2008, 2011, BAUCH et al. 2009a, 2009b, 2011, HÖLEMANN et al. 2011). A vorticity index (DMITRENKO et al. 2005), calculated as the numerator of the finite-difference Laplacian of sea level pressure (SLP), and a trajectory index, based on the simple Ekman model for the surface Lagrangian particles (BAUCH et al. 2011), were used to relate, with the help of certain simplified mathematical relationships, the state of the atmosphere in summer with the trajectory of the fresh river water propagation.

Our study is based on three-dimensional modelling. It is motivated by the realization that the Laptev Sea variability results from the combination of different processes, characterized

by spatial and temporal variability, and therefore, the simulation results, based on three-dimensional high-resolution models, will be very useful in addition to hypotheses developed from the observations. To determine how “fine” the resolution of a model must be, a series of numerical experiments using models with different resolutions must be performed. Building on studies based on large-scale modelling of the region (HARMS et al. 2000, PAVLOV & PAVLOV 1999, JOHNSON & POLYAKOV 2001, KULAKOV 2008), we present the results of the Laptev Sea circulation modelling on the basis of a large-scale model of the ocean and sea ice, forced by NCEP/NCAR Reanalysis (KALNAY et al. 1996). We try to understand the following: what determines the circulation system and its variability throughout the year and how does the circulation influence the hydrology fields? What are the possible reasons for the warming of the near-bottom coastal waters? A series of tracers coming from the mouth of the Lena River during the year can serve as an indicator of how volatile the pattern of water circulation is, and how far the riverine waters propagate in different years.

To clarify the processes taking place in the Laptev Sea during a short period, a fine-resolution local model can be used (FOFONOVA et al. 2015). We have simulated the summer period of 2007 and 2008 using a nested shelf ocean model, focused on the Lena River Delta surroundings with an enhanced grid resolution, in order to identify the distinguishing features in the distribution of hydrological characteristics under different modes of atmospheric circulation.

We endeavour to assess the effect of warming of the near-bottom waters on the current state and stability of the submarine permafrost within the ESAS. To do this, we first simulated the subsea permafrost evolution for the last glacial cycle and then we continued the simulation using the near-bottom temperature from our coupled ice-ocean large-scale model.

## NUMERICAL MODELS

### *The large-scale coupled regional ocean-ice model*

When carrying out the basic experiment, we used the coupled regional ocean-ice model (GOLUBEVA & PLATOV 2007, 2009) developed in the Institute of Computational Mathematics and Mathematical Geophysics (Siberian Branch of the Russian

Academy of Sciences). The ocean model is based on the conservation laws for heat, salt and momentum, as well as on conventional approximations: Boussinesq, hydrostatic and “rigid lid”. After the separation of the momentum equations into the external and internal modes, the barotropic equations are expressed in terms of a stream function. When integrating over time, a hybrid explicit-implicit scheme and splitting of physical processes and spatial coordinates are used. The QUICKEST scheme (LEONARD 1979) is employed to approximate advection. Multidimensional extension uses the COSMIC approach (Leonard et al. 1996). The vertical adjustment is considered as a mixed layer parameterization based on the Richardson number (GOLUBEVA et al. 1992). No-slip boundary conditions are used at the solid boundaries. The specified mass transports at open boundaries and river inflows are compensated by transports through the outflow boundary at 20° S.

The ocean circulation model has been coupled with the CICE v3 model of the thermodynamics of elastic viscous-plastic ice (HUNKE & DUKOWICZ 1997) and multi-category sea-ice thermodynamics (BITZ & LIPSCOMB 1999). Sea-ice advection utilizes a semi-lagrangian scheme (LIPSCOMB & HUNKE 2004). The fast ice parameterization is the most simplified approach, and ice velocity was set to zero in the shallowest part of the Laptev and East Siberian Seas (depth <30 m) for the period of 30<sup>th</sup> October to 1<sup>st</sup> June.

The model domain includes the Arctic and the Atlantic Ocean north of 20° S. The grid resolution for the North Atlantic is chosen to be 0.5° x 0.5°. At 65° N, the North Atlantic spherical coordinate grid is merged with the displaced poles of the Arctic grid. The horizontal grid size in the Arctic varies from 10 to 25 km with an average grid spacing of about 18 km. The model version used here has 38 unevenly spaced vertical levels with a maximum resolution of 5 m in the upper 20-meter layer. A minimum depth of the shelf zone is taken to be 20 m.

The model takes into account the inflow of the 52 largest rivers in the region, among which are the Siberian rivers: Yenisei, Ob, Lena, Indigirka, Olenek, Yana and Kolyma. Data on the average seasonal runoff from these rivers were obtained from measurements of hydrological stations (VÖRÖSMARTY et al. 1998). In addition, according to the estimates by AAGAARD & CARMACK (1989), the total runoff of continental waters in the Arctic is approximately 1.3 times greater than that of the main rivers. Therefore, to obtain the whole picture, the discharge of the above-mentioned rivers was increased by 1.3 times, including those of the Atlantic basin. The rivers’ freshwater flux was calculated on the basis of the assumption that river water has zero salinity. We included the Lena River runoff considering only one channel, located in the east of the delta. In the basic experiment, we did not consider the temperature of the river water entering the shelf zone.

The model is forced by the NCEP/NCAR Reanalysis data (KALNAY et al. 1996). The initial distribution of temperature and salinity fields corresponds to the climatic data PHC (STEELE et al. 2000) for the winter period.

### *Particle tracer model*

In order to numerically track the distribution of the river water we used the method of Lagrangian particles. The particles are individually and periodically emitted in the region of a certain source and move within the numerical domain with a model velocity. To calculate the position of a particle  $\vec{r}$  moving with a certain velocity  $\vec{v}$  from the initial point  $\vec{r}_0$ , one can use the explicit advection equation in the form of Lagrange:

$$\vec{r} = \vec{r}_0 + \vec{v} \cdot dt,$$

where the velocity  $\vec{v}$  is an interpolant of the model velocity field at a point  $\vec{r}_0$ , and  $dt$  is a model time step.

The advective motion of particles is also accompanied by the diffusion, which is considered as a stochastic process. The position of the particle caught in the layer of convective or wind mixing is also stochastically determined on the basis of a uniform distribution in the mixed layer. A particle of any river runoff was deployed in a way that it represents the volume  $V_0 = 0.6859 \text{ km}^3$ . This means that the time interval between two successive particle releases is determined as  $\Delta t = V_0/R(t)$ , where  $R(t)$  is a current river discharge rate in  $\text{km}^3/\text{s}$ .

### *The regional nested model*

A number of processes that have an important influence on the dynamics cannot be correctly described within a large-scale model. Such processes include the propagation of topographical and coastal trapped waves and tides. The movement of these waves causes surface level disturbance that leads to cracks in the ice cover and contributes to relieving the stress in the ice field. A high horizontal resolution in areas of steep continental slopes is sufficient for a satisfactory description of these waves. In addition, a detailed resolution near the Lena River delta is also necessary for a correct description of the interaction of riverine and marine waters. We used a radial numerical grid with the centre in the Lena Delta. The radial distance ranged from 850 m near the Lena Delta, to 3 km in the areas most remote from the delta. The distance between the grid points along the circumference increased from 450 m to 8 km. The model grid for this region is presented in Figure 2.

To describe the dynamics of the shelf water, a detailed grid resolution is required not only for the surface, but also for the bottom boundary layer. In addition, the model should allow for vertical displacements of the sea surface, i.e., the “rigid lid” condition, which is used in our large-scale model, is unacceptable for a regional shelf model. Among the ocean models satisfying these requirements, the sigma-coordinate model, developed in Princeton University (POM) has been selected as the most suitable (BLUMBERG & MELLOR 1987).

The problem of downscaling needs to be addressed both in terms of accounting for the large-scale distribution within a nested model, and to account for the combined influence of smaller-scale processes in the large-scale dynamics. The approach discussed by PLATOV & KLIMOVA (2014) was used here. This approach uses diffusion terms in a set of equations not for predicted fields but for their deviations: (a) from large-

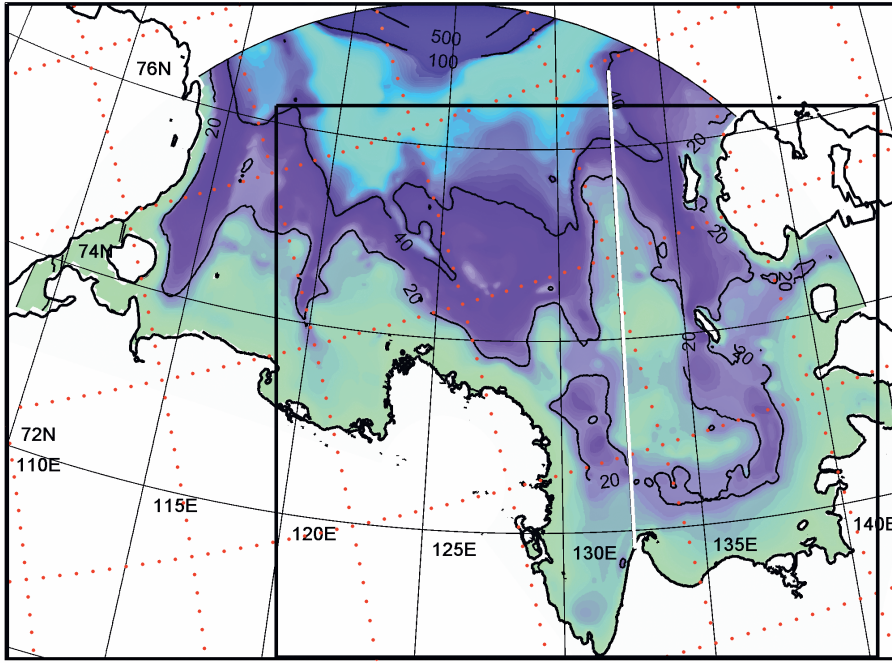


**Fig. 2:** The Laptev Sea nested regional model domain. The map of the bottom topography (depth in m) is adapted from IBCAO (JAKOBSSON et al. 2012). The rectangular frame indicates the area depicted in subsequent figures. Red dotted lines represent the grid lines of the large-scale model of the Arctic and the North Atlantic Ocean (1 in every 10 lines is shown). The white line represents the position of a cross-shore transect to be discussed later.

**Abb. 2:** Übersicht über die modellierte Region der Laptewsee. Karte der Bodentopographie (Tiefen in m) nach IBCAO (JAKOBSSON et al. 2012). Der quadratische Rahmen beschreibt das in den folgenden Abbildungen dargestellte Gebiet. Rote Punkt-Linien stehen für die Netzlinien des großmaßstäblichen Arktis-Nordatlantik Modells (1 von 10 Linien ist gezeigt). Die weiße Gerade zeigt die Lage des später diskutierten küstensenkrechten Schnittes.

scale distribution in the nested model, and (b) from integrated nested model values in the large-scale model.

The coordinate lines of the nested model do not coincide with the coordinate lines of the large-scale model, so the following interpolation formula was used to solve the problem of data transfer from one grid to the other:

$$\tilde{\psi}_i = \frac{\sum_j C_{i,j} \psi_j}{\sum_j C_{i,j}},$$

where  $\psi_j$  is the value of some variable  $\psi$  at the  $j$ -th node of the original grid,  $\tilde{\psi}_i$  is the resulting value obtained by interpolation at the  $i$ -th node of the destination grid. The weight coefficients  $C_{i,j}$  are calculated depending on the distance  $r_{i,j}$  between any  $j$ -th node of the original grid and the  $i$ -th node of the destination grid by the formula

$$C_{i,j} = \exp\left\{-\frac{r_{i,j}^2}{4R^2}\right\},$$

where  $R$  is the search radius.

The value of  $R$  must ensure the existence of at least three nodes of the original grid within this radius. The summation is done over  $N$  nearest nodes. In order to facilitate interpolation from one grid to another during the model run, pre-calculated interpolation coefficients  $C_{i,j}/\sum_j C_{i,j}$  were used. Additionally, it was assumed that  $N = 16$  and  $R$  is equal to the local grid spacing of the large-scale model.

In contrast to the large-scale model, where the discharge of river water passed through one channel, the local shelf model uses a system of 22 channels, distributed along the coast of the Lena Delta. Simulation data of the hydrological and thermal regimes of the Lena River were used to define freshwater and heat flux in the river mouth at the entrance to the Laptev Sea (SHLYCHKOV et al. 2014).

## LARGE-SCALE NUMERICAL RESULTS

The basic experiment simulates the large-scale variability of the Arctic Ocean circulation and sea ice state, caused by variability of the atmosphere in the period from 1948 up to 2014. The grid resolution of the model, as related to the shelf zone, does not allow the recovery of certain features of circulation and hydrology, but it does reveal characteristic features and physical mechanisms of the large-scale variability of the region.

The results of the three-dimensional simulation present the space-time variability of the hydrological fields on the Siberian shelf and they show that the variability of the Laptev Sea circulation is quite large. The use of the Lena River particle tracers in our numerical model allows us to follow their path and get an idea of circulation variability. During the numerical experiment, we stored the information about the date of issue and the three-dimensional coordinates of each tracer, which allows us to track the location of any tracer in a certain period. We have chosen three years to show the different variants of the tracers originating from the Lena River propagation. Our model particles were issued within a twelve-month period, starting on the 1<sup>st</sup> of April and finishing on the 31<sup>st</sup> of March the following year (Fig. 3).

### Main features of the Laptev Sea summer circulation

The discharge of river water begins to increase in May when the sea shelf zone is still covered with ice (AARI/ECIMO), which isolates shelf waters from the dynamic effects of the atmosphere. According to the theory of freshwater plume dynamics, the main flow at that moment deviates to the right and propagates along the coastline. In addition, the circulation that was formed in the winter is also involved in the transfer of river water in the spring. This was manifested in our numerical experiments as the initial distribution of river tracers moving

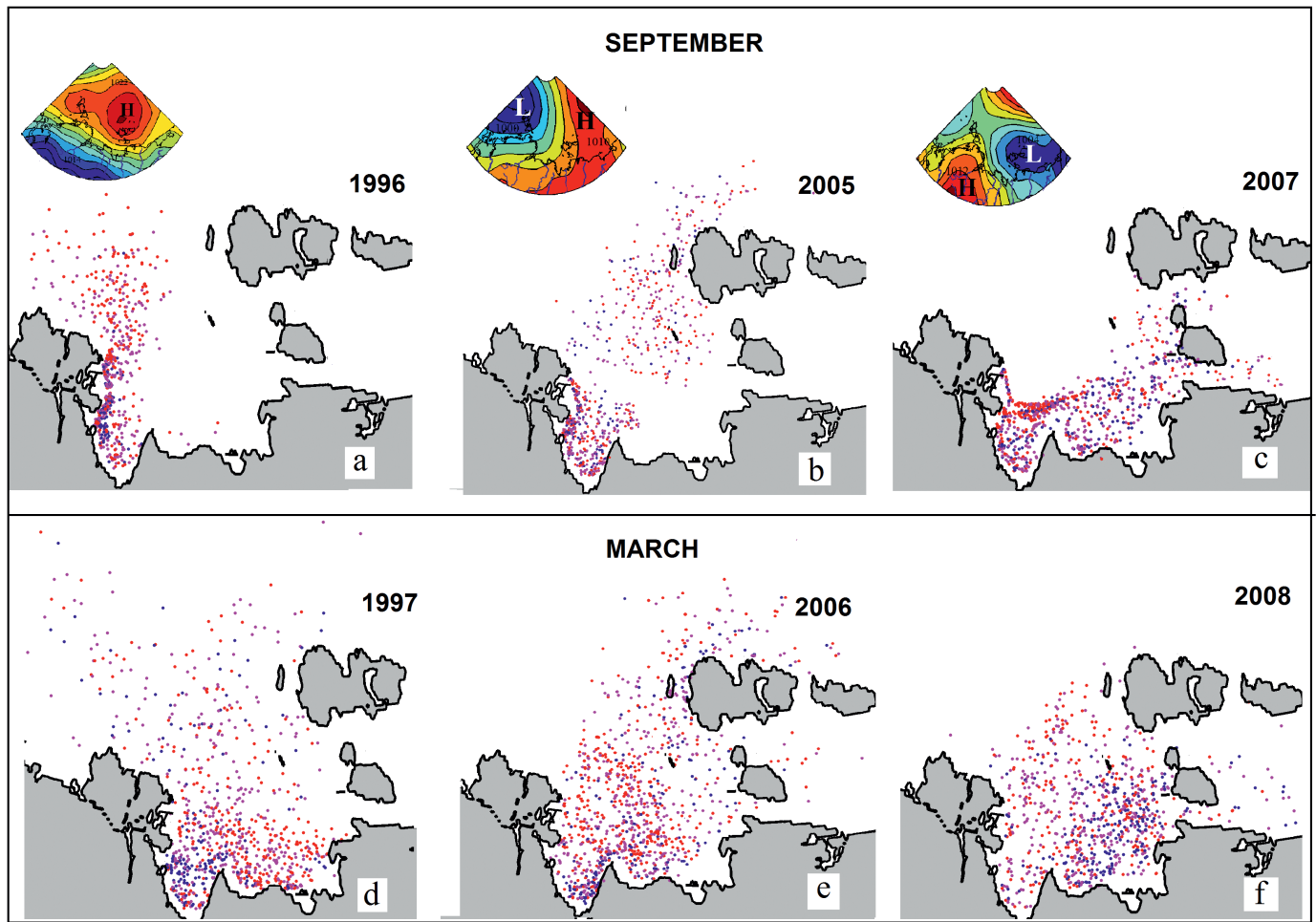


**Fig. 3:** The simulated distribution of tracers originating from the Lena River, starting on the 1<sup>st</sup> of April and finishing on the 31<sup>st</sup> of March the following year. Variability of pathways is caused by the atmospheric dynamics. Upper panel shows the distribution in September, lower panel corresponds to March. Summer 1996 and 2005 correspond to off-shore tracer trajectory, summer 2007 to onshore. The colour of the particles denotes the depth ( $h$ ) of the tracer location: red:  $h < 5$  m; magenta:  $h < 5 - < 15$  m; blue:  $h > 15$  m. Sea level pressure (in mbar) is shown for September of every year.

**Abb. 3:** Simulierte Verteilung der Tracer aus der Lena für den Zeitraum 1. April bis 31. März des folgenden Jahres. Die variable Verteilung spiegelt die atmosphärische Dynamik. Oben: September-Verteilung. Unten: Verteilung; im März. Die Sommer 1996 und 2005 korrespondieren mit ablandigem Transport, der Sommer 2007 mit auflandigem Transport. Die Färbung der Punkte beschreibt die Wassertiefe ( $h$ ) der Tracer-Probe: rot:  $h < 5$  m; magenta:  $h 5 - < 15$  m, blau:  $h > 15$  m. Druck am Meeresspiegel (mbar) jeweils für September.

in a northerly direction, and it is only in June that a lot of tracers appear along the coast.

From the second half of July to September, the circulation of the Laptev Sea in our results is most closely related to the dynamic effects of the atmosphere and a pronounced type of the summer circulation results from the predominance of a certain type of atmospheric forcing. The northerly and westerly winds prevalent over the Laptev Sea in the summer period from June to September tend to cause onshore or alongshore surface water transport (SHPAIKHER et al. 1972, GUAY et al. 2001, DMITRENKO et al. 2005). Following GUAY et al. (2001), these years are known as “onshore” years. In contrast, years with predominantly southerly to south easterly winds, which cause an offshore transport of surface waters, are called “off-shore” years. According to analysis of the observations, the summer circulation of the surface water in the Laptev Sea was characterized as “onshore” in 1993, 1994, 2006 and 2007 and “off-shore” in 1995, 1996, 1999 and 2008 (GUAY et al. 2001, DMITRENKO et al. 2005, 2008, 2011, BAUCH et al. 2009a, 2009b, 2011, HÖLEMANN et al. 2011).

Our simulation, forced by the NCEP/NCAR Reanalysis, has shown that a stable expression of the summer circulation is not frequently formed. The Lena River tracers change the direction of their pathways several times during the summer season and a pronounced offshore or alongshore transport by the end of summer is evident only in certain years. Figure 3a-c demonstrates the summer distribution of particles at the end of September.

We assume that we often simulated the offshore mode, for example, in 1995, 1996, 1999, 2005 and 2008, although evaluating the distribution of the tracers in late September, often we can see the consequences of the circulation mode changing. The pattern for 1996 (Fig. 3a) shows the particles located to the north and northwest of the Lena Delta. We also see several tracers near the coastline and some particles in the Buor Khaya Bay as a remnant of redistribution of the tracers transported by the density-driven flow in spring. The conditions associated with offshore transport prevailed throughout September 1996 and contributed to the large amounts of fresh water spreading around the Lena Delta (Fig. 4a, d).

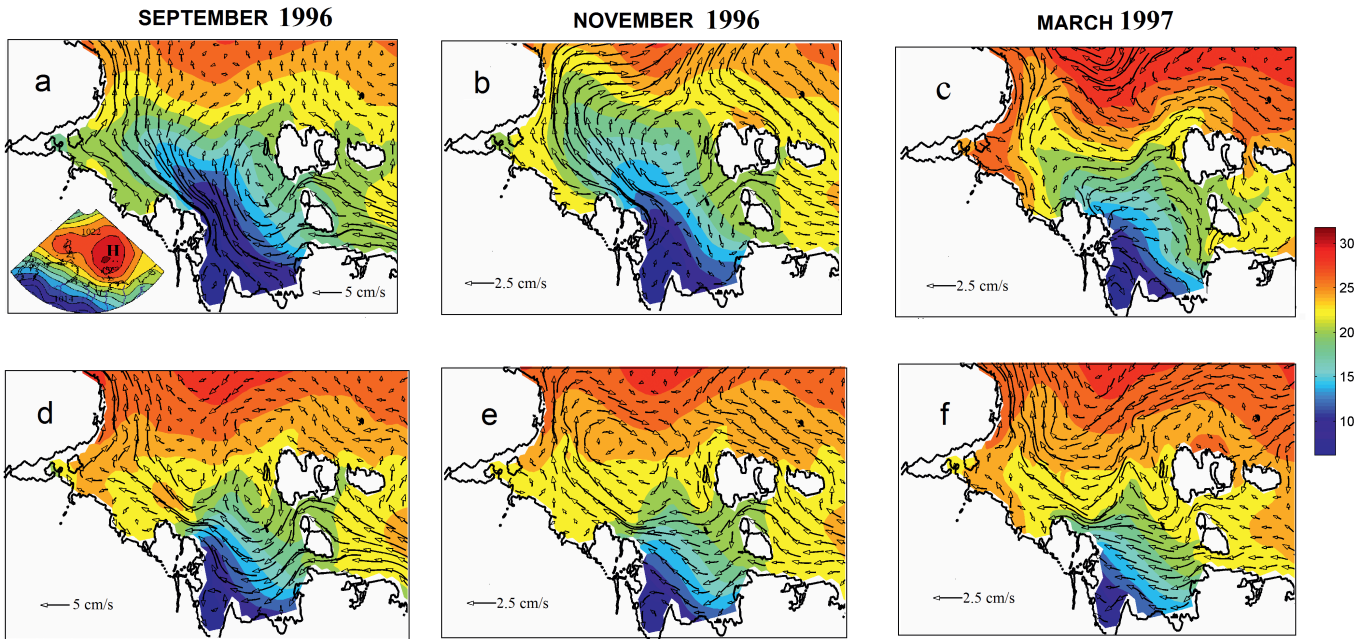


**Fig. 4:** Large-scale simulation of the Laptev Sea circulation in 1996 and 1997. Monthly mean fields of salinity (psu), and velocity for September (a, d); November (b, e); and March (c, f). The upper panels show the distribution averaged over the upper 12.5 m, the lower panel shows from 12.5 m down to 100 m. Sea level pressure (in mbar) is shown for September.

**Abb. 4:** Großmaßstäbliche Simulation der Zirkulation in der Laptevsee April 1996 bis März 1997. Dargestellt die monatlichen Werte für Salinität (psu) und Geschwindigkeit im September (a, d), November (b, e) und März (c, f). Oben: Die durchschnittliche Verteilung in den oberen 12,5 m; unten: durchschnittliche Verteilung von 12,5 m bis 100 m Tiefe. Druck am Meeresspiegel (mbar) jeweils für September.

The September 2005 tracer distribution (Fig. 3b) shows that as a consequence of offshore northward transport in August, the model tracers have reached the area of the Laptev Sea continental slope but the intensive westerly winds in September force a lot of the tracers back to the central shelf region. A group of the particles are also seen in the Buor Khaya Bay.

The model simulates a pronounced alongshore mode in summer 2001 and 2007, the tracers are concentrated close to the Lena River mouth and along the coastline (Fig. 3c) and some of them enter the East Siberian Sea through the straits between the islands. In 2007 the eastward flow is steadily present throughout the summer season in our large-scale model (Fig. 5a, d). The salinity front develops in the surface

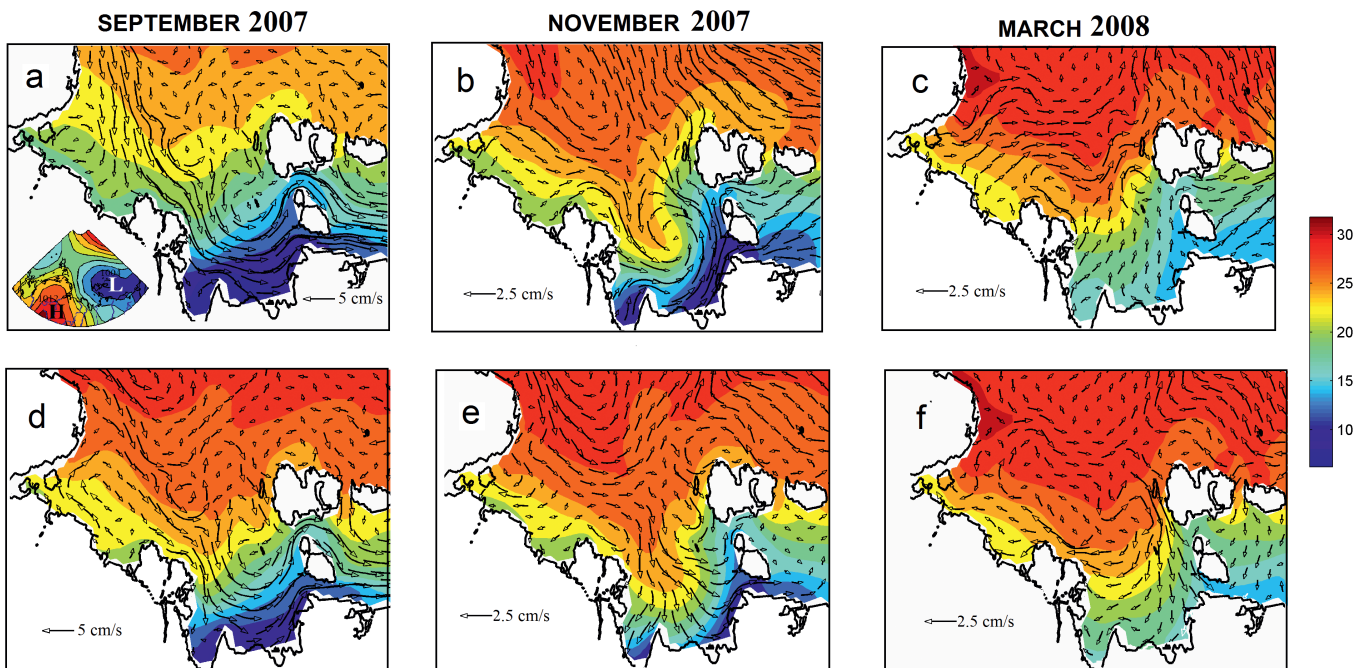


**Fig. 5:** The same as in Figure 4 but for the year April 2007 until March 2008.

**Abb. 5:** Wie in Abbildung 4 jedoch für das Jahr April 2007 bis März 2008.

waters and spreads along the coast of the Laptev and the East Siberian seas. In September, our model simulates a local cyclone in the eastern part of the Laptev Sea, and the salinity increases in the central part of the Laptev Sea due to the influx of more saline water from the Arctic zone.

### *Main features of the Laptev Sea winter circulation*

Further analysis of the numerical results involved examining the patterns of further transport of the tracers for selected years and this revealed the winter particles location at the end of March in the following year (Fig. 3d-f). A common feature of the tracers' distribution obtained in the next winter for three variants with differing summer circulation modes, was that the bulk of the tracers remained within the eastern part of the Laptev Sea shelf. The winter distributions differed in their details, in particular in terms of the areas where the particles were located. This indicates that the circulation patterns differ in the autumn–winter period for the selected years. Different concentrations of particles in the surface and near-bottom layers, shown in Figure 3 by colours, indicate a three-dimensional pattern of water circulation.

To understand the principles of the formation of winter circulation, we return to the state that was formed in the late summer period for various circulation regimes and distinguish between the two most different states, “expressed offshore” and “expressed onshore”.

An example of the expressed cyclonic (“alongshore”) circulation pattern, known from observations (BAUCH et al. 2010, HÖLEMANN et al. 2011), was simulated in 2007 (Fig. 5a). The cyclone intensifies in November and the salinity front becomes oriented along the New Siberian Islands (Fig. 5b). At the same time, the Lena River discharge is sharply reduced and fast ice is formed which isolates the shelf water from the dynamic effects of the atmosphere. Under these conditions, water circulation is caused by pressure gradients, the main contribution to the formation of which is made by the distribution of salinity. In the near-bottom layer, the influence of flows from the adjacent regions increases, emanating from the central part of the basin (Fig. 5e).

In winter, the flow through the straits contributes to the gradual decrease of the salinity gradient (Fig. 5c). A wide off-shore flow is formed in the upper layer. In the near-bottom layer the model simulates an anticyclonic circulation (Fig. 5f), the northern branch of which coincides with the eastward flow of waters along the continental slope. The eastern part provides a transport of outer shelf waters shoreward, as return flow to off-shore directed surface flux near the New Siberian Islands. The cycle is closed by a westward flow along the Lena Delta. The resulting pattern of circulation explains why most tracers remain within the eastern part of the Laptev Sea (Fig. 3f). The upper layer traces were mostly transported far to the north, while the tracers of the bottom layer remained localized in the south-eastern part of the Laptev Sea. There were few tracers left in the Buor Khaya Bay, especially the bottom ones, since they were transported eastward or raised to the upper layers and transported to the north by the winter currents.

The expressed “offshore” circulation pattern is implemented with the model during the summer period of 1996 (Fig. 4a). The conditions associated with offshore north-westward transport prevailed throughout September 1996 and contributed to the large amounts of fresh water locked in around the Lena Delta by the end of summer. After fast ice formation, the density gradient brings about the formation of the anticyclonic circulation, including the central and eastern part of the sea, and this structure is retained throughout the winter period of 1996-1997 (Fig. 4b, c). The near-bottom circulation is defined by the westward flow from the East Siberian Sea, around the southern part of the Laptev Sea (Fig. 4e, f).

We have analysed our simulation results for the period of 1985 to 2014 and revealed that other states, formed when the offshore circulation mode intensively changed in September and October, show an intermediate variant in winter between these two states described above.

The simulation results show that the salinity formed during the autumn period under the influence of the wind, persists for a long period in winter and gradually change due to the contact with the adjacent water areas. This assumption, made during the analysis of the spatial and temporal variability of our results, is confirmed by the conclusion made by DMITRENKO et al. (2010) based on observations. They noted the similarity detected between general patterns of the winter surface salinity fields and those from the previous summer, and suggested that “*patterns in surface hydrography can be maintained through the entire winter season from September to March until main polynya events occur in April–May, and the winter salinity field represents the remnants of the summer field modified by seasonal sea-ice formation*” (DMITRENKO et al. 2010).

### *The Lena River as a supplier of heat into the shelf water*

The riverine water is a significant source of heat for the Laptev Sea, in addition to the surface heat flux. To determine the effect of heat supplied by river waters in our model, an additional numerical experiment was carried out in which the Arctic rivers' temperature data (WHITEFIELD et al. 2015) were used at the boundary corresponding to the mouths of the Siberian rivers. To understand spreading of the heat associated with the incoming river water over the shelf, we defined arrays of temperature anomalies as the difference between the three-dimensional monthly averaged water temperature for this experiment and the same arrays for the basic experiment. To analyze the spreading of these anomalies, the eastern part of the Laptev Sea was divided into four subregions (Fig. 1). Averaging over each subregion provides a time series showing the appearance and the life-time of monthly mean temperature anomalies occurring in different years. Figure 6 represents temporal variability of the anomalies in these regions. The highest values of monthly mean temperature anomalies (2.5 °C) are obtained in June, in Region I located in the vicinity of the eastern output of the Lena River and to its south. A maximum temperature anomaly is recorded at a depth of 5 m, which corresponds to the mixing process of the sea and the river waters. Temperature anomalies, seen in Regions II, III or IV, result from the predominant directions of the water flow, i.e. northwest, alongshore or northeast, respectively. The surface maximum in Region III in July is caused by the Yana River heat flux.

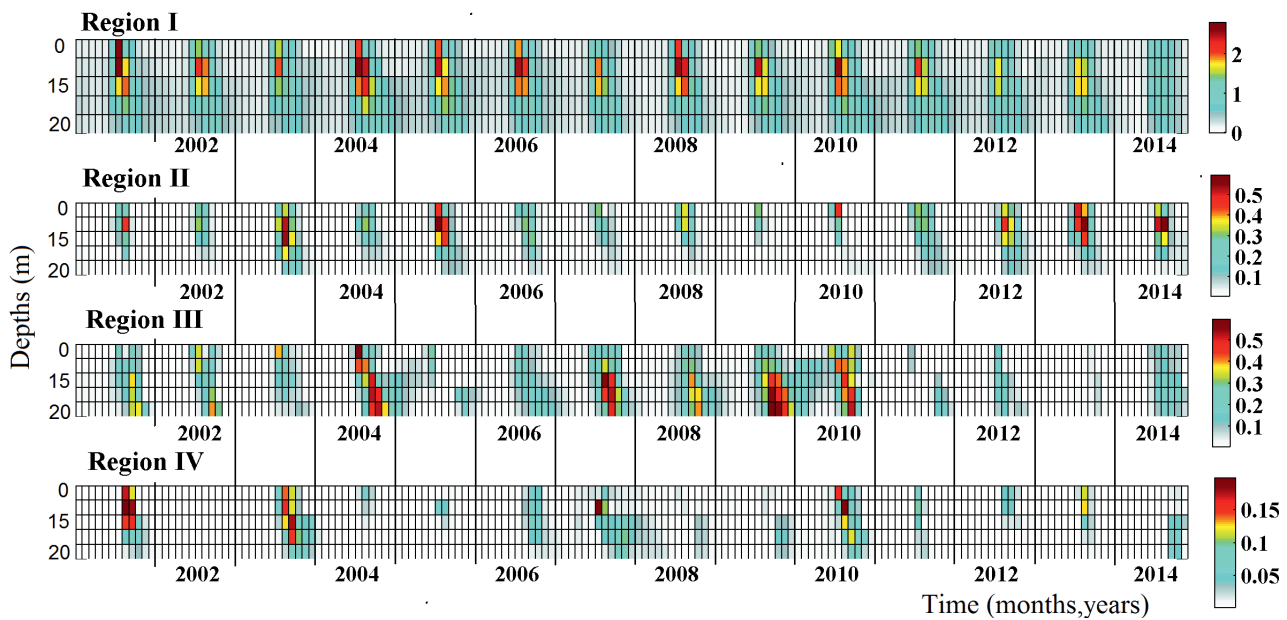


**Fig. 6:** Temporal variability of the temperature anomalies ( $^{\circ}\text{C}$ ) associated with the incoming Lena River water. Temperature anomalies are averaged over subregions, marked in Figure 1.

**Abb. 6:** Zeitliche Variabilität der Temperatur-Anomalien ( $^{\circ}\text{C}$ ) in Zusammenhang mit dem Abfluss der Lena. Dargestellt sind Durchschnittswerte der in Abb. 1 markierten Subregionen I bis IV.

In some years the second maximum exists, resulting from the Lena River water reaching Region III. More significant for this region is an anomaly occurring every year in the near-bottom layers in the autumn months. The signal, showing the warming of near-bottom waters due to the arrival of heat supplied by river waters, is noticeable in Region II (central shelf) in 2003, 2005, 2011, 2012 and 2013 from August to December. The observations for the 2012/2013 period provide evidence of warming near-bottom waters in the Laptev Sea central shelf, which maintained positive temperatures for  $\sim 2.5$  months, reaching a maximum of  $+0.6^{\circ}\text{C}$  by mid-January 2013 (JANOUT et al. 2016). The reason for this warming could be anomalous summer surface waters and warm river waters that were mixed and advected northward on the central shelf.

The highest values of the temperature anomalies in the near-bottom layer were obtained in Region III, near the coast. Our numerical model shows that this heat comes from Region I with the coastal eastward flow, which is consistently simulated in the autumn period. Consistent with the picture of temperature anomalies, monthly near-bottom temperature (Fig. 7) shows continuous near-bottom warming of the Laptev Sea waters in the vicinity of the eastern output of the Lena River (Region I), in the coastal zone (Region III) and in Region IV (after 2000). Region II is the most stable.

In an assessment based on observational data, DMITRENKO et al. (2011) showed that the sea-ice melting due to positive temperature anomalies of the polar atmosphere, together with eastward flowing riverine water, results in bottom layer freshening and warming during the cyclonic mode of the atmosphere circulation. A dramatic warming of near-bottom waters ( $2.1^{\circ}\text{C}$  in the period from 1984 to 2009) over the eastern Siberian coastal zone, recorded in summer hydrographic data for 1920-2009 was attributed to enhanced summer cyclonicity (DMITRENKO et al. 2011).

#### DETAILS OF 2007 AND 2008 SUMMER CIRCULATION

The response of the water dynamics to the summer mode of the atmospheric circulation can be clarified using the nested high-resolution model. Studying the Lena River freshwater spreading, we considered the simulation period from May to September in 2007 and 2008.

The fine-resolution simulation of summer 2007 shows the development of the Laptev Sea circulation which is characterized as a persistent alongshore circulation pattern. We show a picture of the monthly averaged circulation fields to reveal the most intensive currents simulated. Even though many particulars are missed due to the coarse representation of the figure, some details attract attention. The most prominent features in the circulation picture for June and July are a buoyancy-driven alongshore current, moving eastward from the mouths of the Lena Delta and Yana River (Fig. 8a, c), which passes through the straits and ensures the transport of water into the East Siberian Sea, and a vortex flow, which extends from the Lena Delta channel to the north. The northward flow is not forced by the atmospheric circulation or ice drift, its trajectory corresponds to the location of the 20-m isobath (Fig. 2). A northeastward flow, the location of which coincided with the deepening of the shelf region, was often obtained in the large-scale model results for the winter and spring periods but vortex behaviour was never observed in the large-scale results.

The atmospheric regime in the ice-free period of August and September 2007 was cyclonic with low sea-level pressure north of the Laptev Sea. Persistent westerly winds resulted in the onshore circulation pattern deflecting freshwater plumes of the Lena River to the east, forming the coastal current (WEINGARTNER et al. 1999). The monthly averaged fields of surface currents, obtained in September 2007, are most similar in the large-scale (Fig. 5a) and fine-resolution experiments

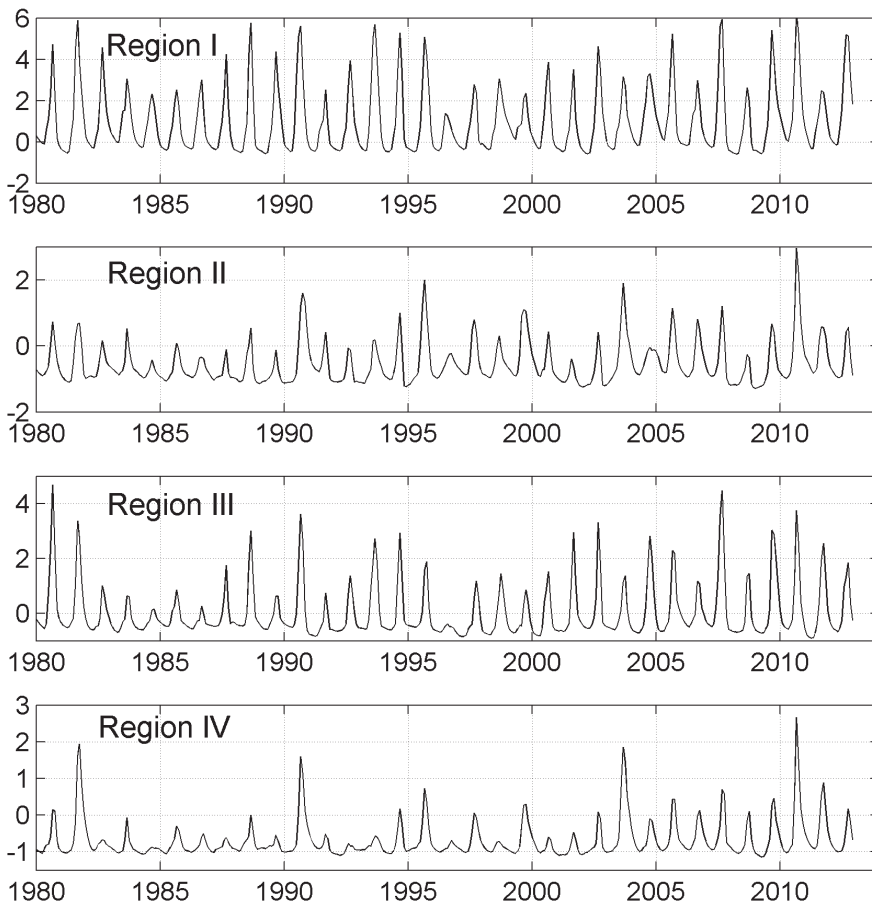


**Fig. 7:** Temporal variability of the near-bottom monthly temperature (°C) averaged over the subregions marked in Figure 1 for the period 1980-2014.

**Abb. 7:** Zeitliche Variabilität der monatlichen bodennahen Temperatur (°C) dargestellt für die in Subregionen I – IV (vgl. Abb.1).

(Fig. 8d). This indicates that the Ekman component provides the largest contribution in the surface layer velocity during ice-free periods. The differences between the large-scale and the fine-resolution results are clearly seen from the comparison of Figures 5a and 8d, representing the simulated surface salinity distribution in September. The additional channels of the Lena River, included in the fine-resolution model, redistributed the Lena River run-off along the Lena Delta boundary. A narrow band of fresh water (salinity less than 5 psu) encircling the delta (Fig. 8d), and the sharp salinity gradients near the coastal line, are the most striking differences between the two simulation results. Fine-resolution simulations (Fig. 8c, d), show the vortex nature of fresh water propagation, which is seen in the salinity field, even in time-averaged distributions for both July and September. The largest amounts of the freshest waters are concentrated in the western part of Bour Khaya Bay, in contrast to Figure 5a, where the freshest waters are seen in the eastern part of the Bay and along the coast.

A map obtained on the basis of the observed surface salinity (DMITRENKO et al. 2010) shows that the Lena River outflow was forced to move alongshore towards the East Siberian Sea in September 2007. It also indicates that the lowest salinity was in the Bour Khaya Bay, which is consistent with our simulation. The observations are absent in close proximity to the Lena Delta, so the narrow belt of fresh water that we simulated is not seen on this map. In addition, our simulation results show the surface layer salinification northeast of the Lena Delta from on-shore inflow of saline water. We consider that our salinity distribution (Fig. 8d) is very close to the observa-

tions analysed by DMITRENKO et al. (2010), who reported that in summer 2007, the measured salinity in the surface layer over the eastern Laptev Sea at 74° N was 22-24 psu, which exceeded the climatic mean of  $15 \pm 4$  psu by  $\sim 2$  standard deviations.

Unlike in the summer period of 2007, the simulated circulation of 2008 shows high variability. In June and in the beginning of July 2008, the Laptev Sea in our model was almost completely covered by sea ice, moving under the southward and south-eastward wind. The simulated results show the creation of a negative salinity anomaly east of the Lena Delta and forming an alongshore current, forcing fresh water further to the east (Fig. 9a,c). As in 2007, the topography dependent northward flow is present. From the middle of July to the middle of September 2008, the atmospheric circulation over the Laptev Sea was preferentially anticyclonic. Westward and north-westward winds were prevailing, providing freshwater advection of the Lena River and ice melt waters toward the north, excluding short periods of strong eastward winds at the end of July and the third decade of August. An anticyclonic circulation cell was simulated during this period (Fig. 9b). One of the branches of this circulation is the northward flow, allowing the simulated circulation situation of summer 2008 to be considered as “offshore”. The eastward flow moving from the Lena Delta along the coast is also visible in the figure. This flow is stronger in September than in August but less intensive than in 2007.

The surface salinity field obtained as a result of modelling the summer circulation in 2008 (Fig. 9d) differs significantly

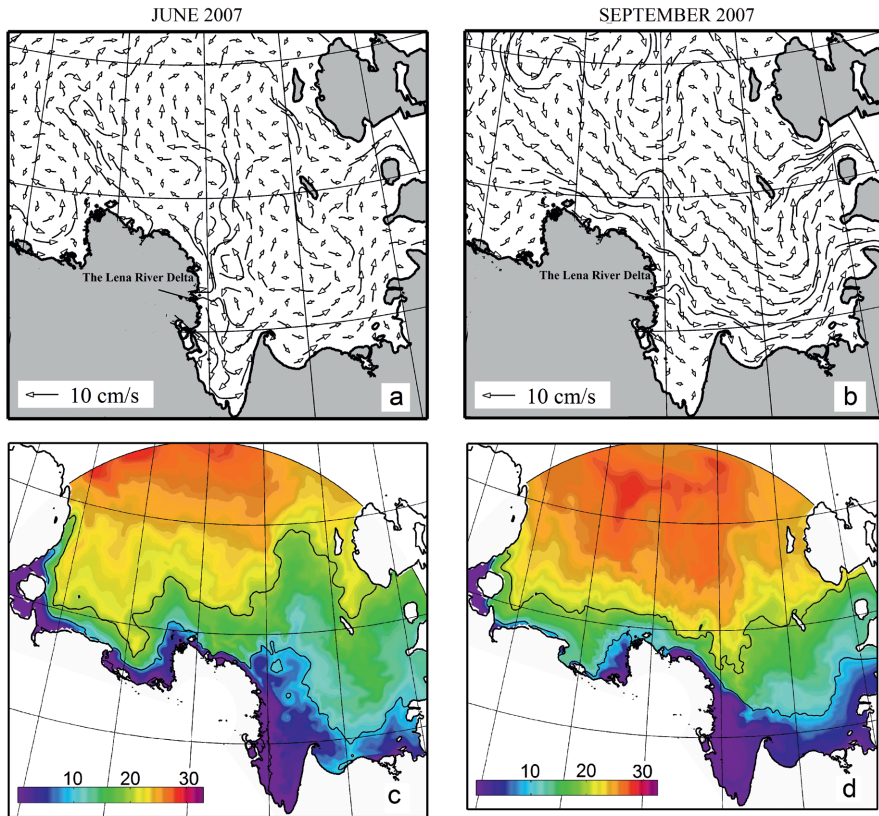


**Fig. 8:** Laptev Sea summer 2007 monthly mean surface circulation (a, b) and salinity in psu (c, d). Left panel shows June, right panel shows September. The simulation is based on the nested regional model.

**Abb. 8:** Laptewsee im Sommer 2007; monatliche Durchschnittswerte der Oberflächenzirkulation (a, b) und Salinität (psu; c, d); links: Juni; rechts: September. Die Simulation basiert auf dem regionalen geschichteten Modell mit unterschiedlicher Auflösung.

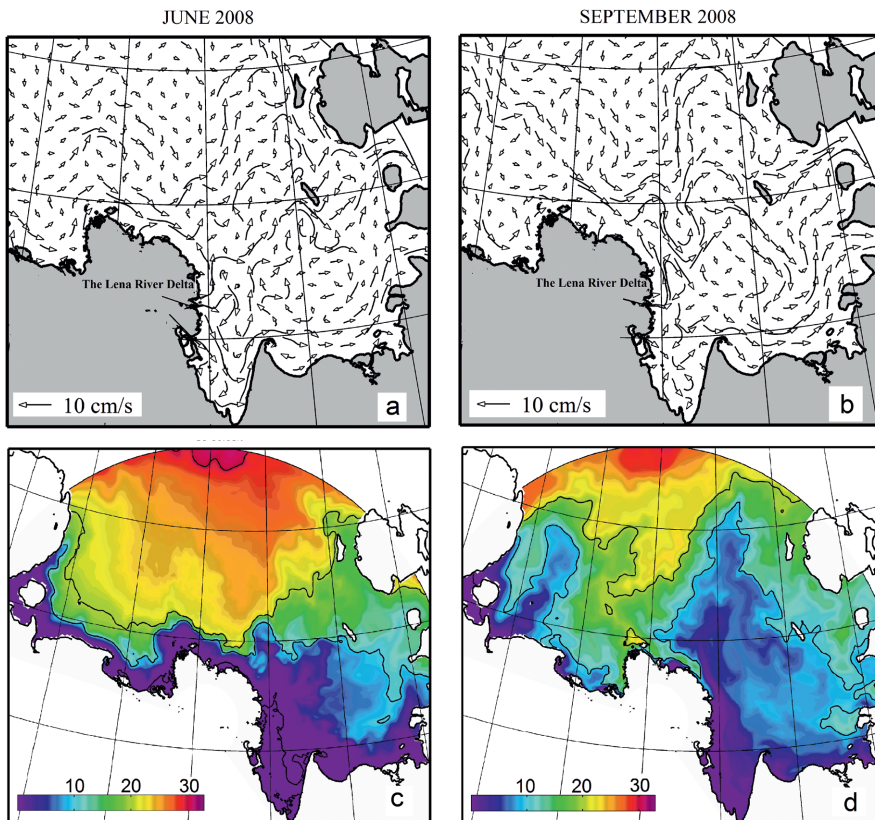


**Fig. 9:** The same as in Figure 8 but for summer 2008.

**Abb. 9:** Wie in Abbildung 8 jedoch für Sommer 2008.

from the analogous field for 2007 (Fig. 8d). We would like to stress that the surface salinity pattern is highly variable within the season. Northward flow in summer 2008 contributed to the freshwater transport to the region of the outer continental shelf. Extensive anticyclonic circulation promoted the freshwater spreading over the eastern part of the sea. Some amounts of freshwater are concentrated in the most southern part of the sea, reflecting the existence of an alongshore current. Strong onshore winds in the second half of September 2008 very rapidly deflected a fresh water plume to the south. As for 2007, the gradients in the salinity field are much sharper than in a smooth large-scale picture. Our modelling results are in agreement with the salinity distribution obtained on the basis of observations for summer 2008. DMITRIENKO et al. (2010) noted a substantial surface layer freshening of  $\sim 7$ -10 psu in summer 2008, resulting from the dominant along-shore winds towards the west over the East Siberian Sea, and the on-shore northerly winds over the Laptev Sea in the anticyclonic regime locked the riverine water in the vicinity of the Lena Delta. There are some discrepancies between our model's salinity and observed salinity distribution. The most visible is the difference in the border of the freshwater plume propagating northward. In our results the plume is wedge-shaped, whereas according to observations it occupies a wider area, extending westward up to  $125^\circ$  E.

The Lena River plume dynamics in the summer 2008 were simulated by FOFONOVA et al. (2015) using the fine-resolution numerical model with horizontal resolution 0.4-5 km. In general, our results in modelling the variability of circulation and the trajectory of propagation are in good agreement. The apparent differences in the surface salinity field refer to the insufficient spread of the plume in the westerly direction in our simulation, unlike the results of FOFONOVA et al. (2015). Possibly this is due to the NCEP/NCAR wind stress which was used to force our model. To obtain the freshwater plume propagation most consistent with observations, FOFONOVA et al. (2015) used the forcing derived from the ECMWF operational atmospheric model because of its higher spatial resolution. They also performed an additional experiment forced by the NCEP-DOE Reanalysis 2 and revealed that in this experiment the spread of the offshore plume was rather limited.

The redistribution of the temperature and salinity fields occurs according to a change in the flow field. The vertical sections of temperature and salinity fields (Fig. 10) allow us to distinguish some features of the process. Water circulation, which was formed in the summer of 2007, contributes to an increase in the vertical mixing in the coastal area (see Fig. 10). Onshore winds generate across-shelf Ekman transport of more saline waters from the central part of the sea, and the fresh water concentration in the coastal domain. Considering normal flow to be zero through the coast, the model simulates downwelling and across-shelf barotropic pressure, resulting in alongshore geostrophic flow. Under these conditions, the stratification of waters is weakened, and the role of wind mixing is intensified. The consequence of this process is the transport of fresh water and heat from the surface to the bottom layer in the shallowest part of the shelf.

In the assessment, based on the summer hydrographic data for 1920-2009 (DMITRENKO et al. 2011), it was shown that in 2007, the near-bottom layer temperature of the Laptev Sea

coast was at its maximum ( $\sim 5.9^\circ\text{C}$ ) for the entire period of field observations.

In June and July 2008, one can see a deepening of the temperature and salinity contours near the coast. This corresponds to a cyclonic flow of the alongshore current, as mentioned previously. In the central part of the sea, a temperature maximum is situated in the subsurface layer, in contrast to the salinity minimum, which is at the surface. The source of this heat is the Lena River in June when the central part of the shelf is still covered with ice. Warm and fresh river waters, being mixed with cold and salty sea waters, sink to the level which corresponds to their density. In August, the maximum water temperature is already at the sea surface due to atmospheric heating. Further development of the anticyclone brings about the formation of the fresh water flow to the north, as is evident from the distribution pattern in August. In contrast to the 2007 situation, sea waters became stably-stratified and this prevents vertical mixing. In the second half of September 2008, in addition to the cooling at the sea surface, a switch of the atmospheric circulation to a cyclonic mode enforced the alongshore current and an intensive mixing near the coast. These effects include deepening contours and the formation of a subsurface maximum.

## THE SIMULATION OF THE SUBSEA PERMAFROST

The ocean bottom water temperature is a significant factor affecting the subsea permafrost distribution (DMITRENKO et al. 2011). In this work, we attempt to assess the effect of warming of the near-bottom waters on the current state and stability of the submarine permafrost within the ESAS. First of all, we numerically simulated the subsea permafrost evolution on the Arctic shelf in East Siberia for the last glacial cycle. Next, we numerically simulated the present-day permafrost state on the East Siberian Arctic Shelf, using near-bottom temperature provided by our large ice-ocean model.

The simulation of the offshore permafrost thickness evolution is based on the model for the thermal state of the subsea sediments (MALAKHOVA & GOLUBEVA 2014, MALAKHOVA & ELISEEV 2017). This model is used to solve the one-dimensional heat equation in the sediment column with a mixed boundary condition. At each shelf point, we simulate the temperature of layers containing the permafrost with allowance for the phase change at the interface. The thermal properties of the sediment are taken to be constant. The simulation of the dynamics of the temperature fields within the shelf was carried out for one climatic glacial cycle, i.e., for the last 120,000 years (MALAKHOVA & GOLUBEVA 2014, ELISEEV et al. 2015). The lower boundary is subject to the constant ground heat flux ( $60\text{ mW m}^{-2}$ ). The value used for the geothermal flux from the Earth's interior is the typical value at the East Eurasia Arctic shelf (DAVIES 2013). The temperature at the top boundary is prescribed by the considered climate change scenario. This scenario includes the reconstruction of climatic conditions of the sea regression and transgression. From the beginning of the ocean transgression, we assume the ocean bottom temperature to be  $-1.5^\circ\text{C}$  by 1948 (the start year of NCEP/NCAR Reanalysis). For analysing the sensitivity of the subsea permafrost to the recent warming from 1948 to 2014, we have simulated the sediment temperature based on the

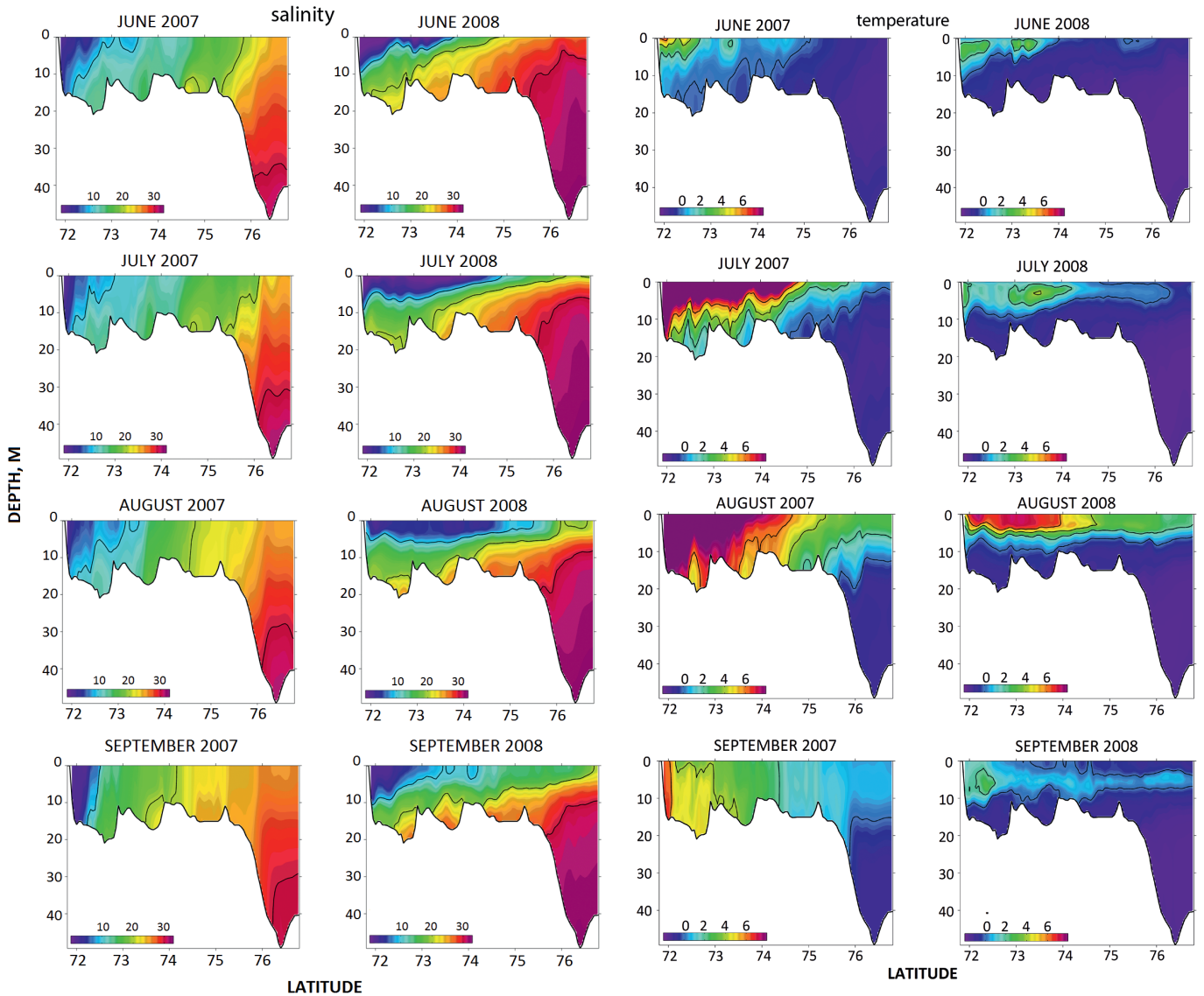


**Fig. 10:** Cross-shelf transect ( $132.5^\circ$  E) of monthly mean salinity (psu, left) and temperature ( $^\circ\text{C}$ , right). Simulation is based on the nested regional model. Left: summer 2007 (onshore). Right: summer 2008 (offshore). The white line in Figure 2 marks the position of the transect.

**Abb. 10:** Trans-Schelf-Profil ( $132.5^\circ$  E) der monatlichen durchschnittlichen Salinität (psu, links) und monatlichen durchschnittlichen Temperatur ( $^\circ\text{C}$ , rechts). Die Simulation basiert auf dem regionalen geschichteten Modell mit unterschiedlicher Auflösung. Links: Sommer 2007; rechts: Sommer 2008. Lage des Profils entspricht der weißen Geraden in Abbildung 2.

bottom water temperature with the large-scale regional model (Fig. 7).

Earlier, we presented results of the subsea permafrost simulation in the case of sediments not contaminated with salt (MALAKHOVA & GOLUBEVA 2014). Measurements of pore water salinity at the ESAS show that the salinity of the shallow sediments is similar to that of the sea water due to infiltration of saline waters into the surface layer of sediments (NYCOLSKY et al. 2012). Since direct observations of the pore fluid salinity distribution within the near-shore Arctic sediments are scarce, it is necessary to evaluate some of the model parameters. Here we follow a commonly accepted approach (RAZUMOV et al. 2014). The salt saturation of bottom sediments (in ‰) is estimated by the formula,  $S(z) = S_B$  for  $z \leq z_S$ , where  $z_S = \sqrt{D \cdot t_M}$  is the depth of salt penetration,  $t_M$  is the time of the presence of permafrost

under the level of the sea in the case of flood with the beginning of transgression. The coefficient of salt diffusion  $D$  was taken as equal to  $10^{-9} \text{ m}^2\text{s}^{-1}$ , which matched the results from the drilling data from the Laptev Sea (RAZUMOV et al. 2014),  $S_B$  is the distribution of bottom water salinity on the shelf (STEELE et al. 2000). Below the level of  $z_s$ , the salinity is exponentially vanishing at the depth of 30 m. The term “subsea permafrost” is used here to describe the geological strata with temperatures  $\leq T_f$ . The freezing temperature of soils mainly depends on the grain size and salt content. For the simulation, we used the freezing temperature of the soil ( $^\circ\text{C}$ ):  $T_f(Z) = -0.0536 S(Z)$ .

The results of our simulation show the existence of offshore permafrost within the vast Arctic shelf in East Siberia. The permafrost depth strongly depends on the shelf water depth. The distribution of the submarine permafrost thickness is characterized by the latitudinal zoning. The present-day permafrost lower boundary varied from 180 m to 550 m for the shelf

(Fig. 11a). The simulation results show the subsea permafrost upper boundary deepening down to 24 m (Fig. 11b). Such a depth of thawing of frozen sediments on the top is defined firstly by the salt saturation due to migration of salts as a result of flooding of this part of the shelf by the sea waters. Due to uneven flooding of the shelf, the submarine permafrost upper boundary deepens offshore.

The rise in the temperature of the bottom water also leads to the destruction of the permafrost from above. Deepening of the upper boundary in the period from 1948 to 2014 is only due to the thermal influence. The modelling results show a permafrost upper boundary deepening of  $\sim 0.5$ -5 m from 1948 to 2014 ( $\leq 7.5$  cm yr<sup>-1</sup>) in the shelf (Fig. 11c). We should note that the sea water temperatures in the Lena Delta region are essentially higher than those in the whole shelf region. The mean summer water temperatures at a depth of 10 m are equal to 3-4 °C (DMITRENKO et al. 2011). The thawing from the sea floor occurs in the offshore zone of the Laptev Sea eastward of the Lena River delta. The submarine permafrost degradation from above occurs most rapidly in the near-shore coastal zone of the shelf and in the areas affected by the river outflow (Fig. 11c). To destroy the permafrost layer, a long-term action of the thermal signal is necessary. Therefore, the spatial variability of the permafrost upper boundary position during the period 1948 to 2014 enables identification of the shelf regions with a steady positive temperature of the bottom water.

Observations of the methane concentrations were conducted over a shallow study area located in the southern Laptev Sea, east of the Lena Delta (SHAKHOVA et al. 2010). This area was documented as a high-emissions-activity site serving as a source of methane to the atmosphere. Extremely elevated concentrations of dissolved methane have been observed annually since 2005. In our study, the simulated impact of the bottom water warming on supposed degradation of the subsea permafrost from 1948 to 2014 is not significant for enhancing methane emission from the thawed sediments. The observed methane vents might be related to the processes of much longer time scales, i.e. to the glacial cycles. For example, as a result of thermokarst processes open taliks are formed, and the conditions for releasing methane from the deep layers are generated (NYKOLSKY et al. 2012, MALAKHOVA 2016).

## CONCLUSION

We used numerical modelling to simulate the most important processes related to the circulation of the Laptev Sea and to understand the main physical mechanisms causing the variability in the region. Our large-scale results are based on the coupled ice-ocean model of the Arctic and North Atlantic, forced by the NCEP/ NCAR Reanalysis (KALNEY et al. 1996). The results of our 3-D simulation show that the atmosphere dynamics and sea-ice states are the major factors related to the circulation of the Laptev Sea. However, the bottom topography, the coastline curvature, the presence of the islands and contact with adjacent areas also play important roles. The combination of these factors forms some specific features of the local circulation.

We show that there is a high variability in the Laptev Sea circulation pattern during the year. The pathways of the passive

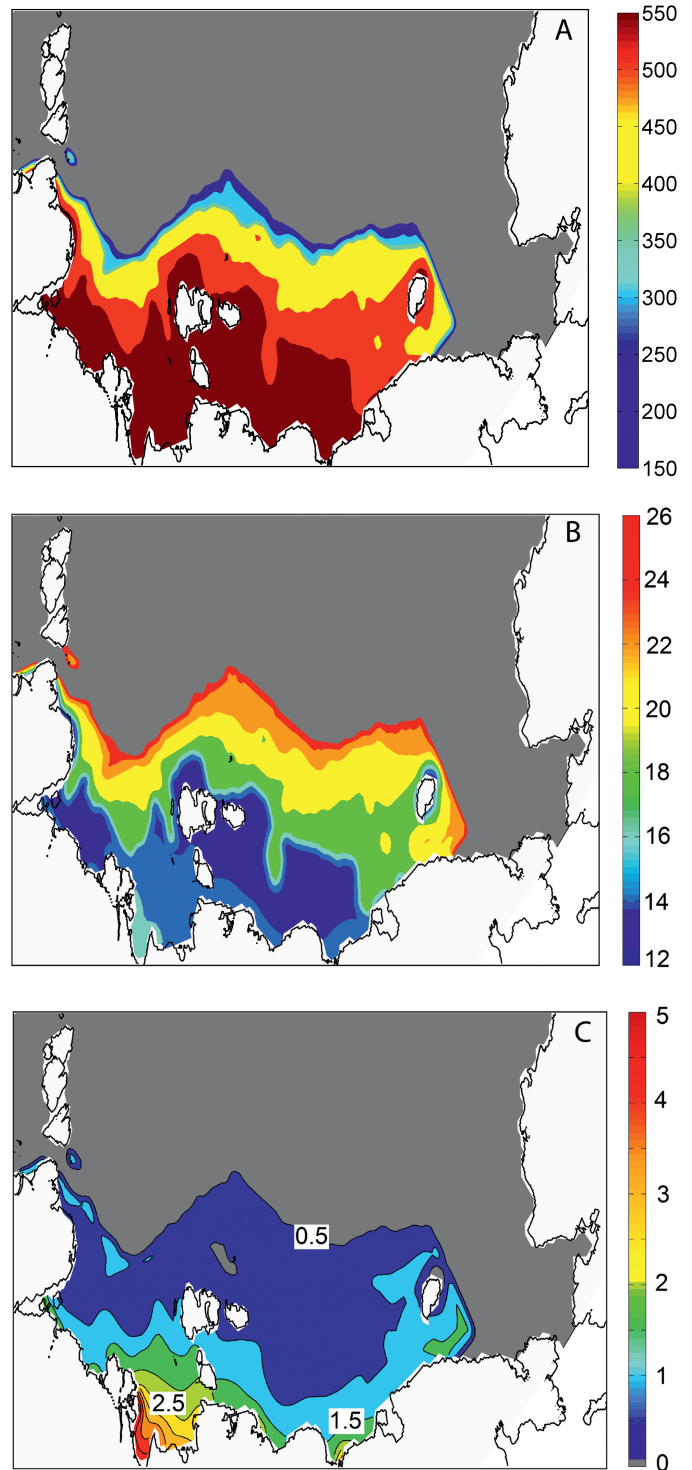


**Fig. 11:** The simulated permafrost of the East Siberian Sea (ESAS). (a): present-day permafrost thickness on the ESAS (m); (b): upper boundary of the simulated permafrost on the ESAS for 2014 (depth in m); (c): deepening of the permafrost upper boundary on the ESAS from 1948 to 2014 (m).

**Abb. 11:** Simulierter Permafrost auf dem ostsibirischen Schelf. (a): Mächtigkeit des Permafrosts (m); (b): Tiefenlage der Obergrenze des simulierten Permafrosts im Jahr 2014, Tiefe in (m); (c): Veränderung der Tiefenlage der Permafrost-Oberkante im Zeitraum 1948 bis 2014 in (m).

tracers, injected in an amount corresponding to the observed monthly mean river runoff of the Lena River, changed their direction several times per year and eventually a bulk of the tracers remained within the eastern part of the Laptev Sea shelf.

The simulated high variability of summer circulation over the Laptev Sea shelf is mainly caused by the difference in the local prevailing wind patterns. In certain years, it is evident that there is pronounced “offshore” or “onshore” and “along-shore” transport. The freshwater from the Lena River produces a very pronounced haline stratification that can be observed in late summer, when the freshwater plume has its largest extent. These results are in good agreement with observations (GUAY et al. 2001, DMITRENKO et al. 2005, 2008, 2011, BAUCH et al. 2009a, 2009b, 2011, HÖLEMANN et al. 2011).

Our study suggests that the response of winter hydrography to the variability of atmospheric circulation is less expressed. The simulation results show that the salinity pattern formed during the autumn period under the influence of the wind persists for a long period during winter and gradually changes due to the contact with the adjacent water areas. This assumption, made during the analysis of the spatial and temporal variability of our results, is confirmed by the conclusions made by DMITRENKO et al. (2010) based on observations.

In winter, the fast ice isolates the Laptev Sea shelf waters from the dynamic effects of the atmosphere, and hence, the circulation is determined by the density distribution, with salinity the main contributor to the formation of gradients. Since fast ice is formed instantaneously in the end of October in our model, the circulation in the Laptev Sea in winter is determined by the density field formed in September and October.

Surface circulation of waters in the eastern part of the Laptev Sea in the autumn period can form the expressed cyclonic or anticyclonic gyre in accordance with the prevailing regime of atmospheric circulation. The cyclonic gyre gradually disappears in winter, due to the weakening of the density gradients caused by contact with the East Siberian Sea and transforms into off-shore flow. The anticyclonic gyre, formed in the model when there is an anomaly of salinity near the eastern shore of the Lena Delta, is fairly stable and its pattern is preserved until the following spring. Most often the model shows intermediate states between cyclonic and anticyclonic circulations and these are determined by mixed atmospheric conditions in the summer period.

In winter, the model often simulates the formation of a near-bottom anticyclonic circulation, the northern branch of which coincides with the flow of waters along the continental slope. The eastern part provides transport of outer shelf waters shoreward as return flow to off-shore directed surface flux near the New Siberian Islands. The cycle is closed by a westward flow along the Lena Delta. The location of the circulation and its extent can vary depending on the density gradient formed in the autumn period and the intensity of the flow of waters from the East Siberian Sea.

We also attempted to study the effect of heat supplied by the rivers to the Laptev Sea shelf in our model. The large-scale model simulated spreading of the temperature anomalies associated with the incoming river water. In summer, the maximum anomalies are found in the surface layer and they propagate by the surface currents forced by the wind. More significant for the Laptev Sea shelf are temperature anomalies occurring every year in the near-bottom layers in the autumn months. The highest values of the temperature anomalies in

near-bottom layer were obtained near the coast. Our numerical model shows that this heat moves with the coastal eastward flow, which is consistently simulated in the autumn period.

The near-bottom circulation obtained in our study does not exclude the possibility of heat transfer in the bottom layer to the region of the central shelf from the area of the continental slope and from the coastal zone. These episodic events were reported in JANOUT et al. (2013) and JANOUT et al. (2016), but consideration of the specific events had been not the focus of our studies. To simulate the winter circulation details of an actual year, our model should be improved by including a more physical model of fast ice and an enhanced model resolution. We are planning to do this as part of a future study.

To analyse in more detail the circulation differences of the Laptev Sea, forced by different modes of the atmospheric dynamics, we used a nested high-resolution model. The simulated fields of temperature, salinity and velocity during the summer periods of 2007 and 2008 are not the direct results of calculations based on a high-resolution model. It would be more correct to call them the refinement of the results of the large-scale model, since for each time step there was a two-way data exchange between the models. Because of using increased resolution both horizontally and vertically, we have obtained a more complex picture of the currents, including the effect of the bottom topography on the circulation and distribution of fresh water.

The cyclonic mode of the atmospheric circulation over the Eurasian Basin, in the summer of 2007, results in the persistent eastward river water pathways along the eastern Siberian coast. We obtained an increase in the vertical mixing in the coastal area resulting in penetration of the heat, stored in the surface layer, to the bottom. The results obtained with our model are in agreement with the assessment based on the observational data (DMITRENKO et al. 2011). In contrast to 2007, summer circulation and surface salinity patterns in 2008 were highly variable within the season. At the end of the summer, our model simulated the extensive northward flow of freshwater and the existence of an alongshore current. The heat flux, penetrating into the near-bottom layers of the shelf zone, was significantly lower than in 2007.

The warming of near-bottom waters on the Laptev Sea shelf, obtained in our simulation and known from observations (DMITRENKO et al. 2011, HÖLEMANN et al. 2011, JANOUT et al. 2013, JANOUT et al. 2016) deserves special attention due to its potential impact on the submarine permafrost, formed during the last glacial cycle, when the Arctic shelf was above sea level. We have numerically simulated the subsea permafrost evolution in the Arctic shelf in East Siberia for the last glacial cycle. The simulated permafrost has a continuous character within the vast ESAS and its thickness is estimated at 180-550 m given the average geothermal flow value of 60 mW m<sup>-2</sup>. The thawing of the permafrost from the top depends on the seawater salinity and temperature near the sea floor. The modelling shows that a significant change in the permafrost depth occurs at the seafloor warming in the Arctic Seas. The simulation with marine salt diffusion shows the upper boundary deepening down to a depth of 12-25 m. The impact of the bottom water warming on supposed degradation of the subsea permafrost from 1948 to 2014, as simulated in our

study, is not significant for enhancing methane emission from the thawed sediments. The submarine permafrost degradation from above is the most rapid in the near-shore coastal zone of the shelf and in the areas affected by the Lena river outflow. Episodic warming of near-bottom waters in the other shelf regions does not lead to additional destruction of the submarine frozen layer, which is explained by the short period of the warming anomalies.

In general, the thickness of unfrozen sediment layers obtained in our simulation for 2014 is consistent with the study by DMITRENKO et al. (2011), where the basic process related to the permafrost evolution in the coastal zone was considered. In addition, we have simulated the spatial distribution of the thickness of unfrozen sediment layers for the East Siberian Arctic Shelf for depths of 10-100 m. To do this we used a model complex describing the redistribution of heat in the atmosphere-ice-ocean-bottom sediments system. This approach enables one to analyse not only temporal changes, as in DMITRENKO et al. (2011), but also spatial changes in the subsea permafrost state on the shelf, as well as to identify areas which are most sensitive to recent and possible future climatic warming in the Arctic. As a result of this study, we can identify the shelf areas where the positive water temperature is the dominant factor affecting the subsea permafrost state at present.

In summary, our conclusions are consistent with DMITRENKO et al. (2011), who stated that the recent methane supersaturation, reported by SHAKHOVA et al. (2010), is not the result of the recent climatic changes in the Arctic, but the result of the continuous degradation of submarine permafrost associated with flooding of the shelf during the last transgression.

## ACKNOWLEDGMENTS

This study is supported by FASO Russia (Grant 0315-2016-0004), RFBR (Grants 17-05-00382A, 17-05-00396A), German Federal Ministry of Education and Research (BMBF, the project “LenaDNM“, 01DJ1400). We also thank AOMIP and the Forum for Arctic Ocean Modelling and Observational Synthesis (FAMOS), funded by the National Science Foundation Office of Polar Programs (awards PLR-1313614, PLR-1203720), for providing travel support to attend the FAMOS workshops and for an opportunity to exchange ideas on Arctic modelling. We thank Markus Janout and an anonymous reviewer for careful reading of the manuscript and helpful comments and suggestions.

## References

- Aagaard, K., Coachman, L.K. & Carmack, E.C. (1981): On the halocline of the Arctic Ocean.- *Deep-Sea Res.* A 28: 529-545.
- Aagaard, K. & Carmack, E.C. (1989): The role of sea ice and other fresh water in the Arctic circulation.- *J. Geophys. Res.* 94(C10):14485-14498.
- AARI/ECIMO Arctic and Antarctic Research Institute, project ECIMO 2017: <<http://www.aari.ru/projects/ECIMO/index.php>> Maps of the Arctic sea ice, [access 15 November 2017].
- Bauch, D., Dmitrenko, I.A., Wegner, C., Hölemann, J., Kirillov, S.A., Timokhov, L.A. & Kassens H. (2009a): Exchange of Laptev Sea and Arctic Ocean halocline waters in response to atmospheric forcing.- *J. Geophys. Res.-Oceans* 114: C05008.
- Bauch, D., Dmitrenko, I.A., Kirillov, S., Wegner, C., Hölemann, J., Pivovarov, S., Timokhov, L.A. & Kassens H. (2009b): Eurasian Arctic shelf hydrography: Exchange and residence time of southern Laptev Sea waters.- *Continent. Shelf Res.* 29(15): 1815-1820.
- Bauch, D., Hölemann, J., Willmes, S., Gröger, M., Novikhin, A., Nikulina, A., Kassens, H. & Timokhov, L. (2010): Changes in distribution of brine waters on the Laptev Sea shelf in 2007.- *J. Geophys. Res.* 115: C11008.
- Bauch, D., Groger, M., Dmitrenko, I.A., Hölemann, J., Kirillov, S., Mackensen, A., Taldenkova, E. & Andersen N. (2011): Atmospheric controlled freshwater release at the Laptev Sea continental margin.- *Polar Research* 30: 1-14.
- Bitz, C.M. & Lipscomb, W.H. (1999): An energy-conserving thermodynamic model of sea ice.- *J. Geophys. Res.* 104(C7):15669-15677.
- Blumberg, A.F. & Mellor, G.L. (1987): A description of a three-dimensional coastal ocean circulation model.- In: N. HEAPS (ed), *Three-Dimensional Coastal Ocean Models*, Amer. Geophys. Union, Washington:1-16.
- Davies, J.J. (2013): Global map of solid Earth surface heat flow.- *Geochem. Geophys. Geosyst.* 14 (10): 4608-4622.
- Dobrovolskii, A.D. & Zalogin, B.S. (1982): *The seas of the USSR*, Moscow University: 1-192. (in Russian).
- Dmitrenko, I., Kirillov, S., Eicken, H. & Markova, N. (2005): Wind driven summer surface hydrography of the eastern Siberian shelf.- *Geophys. Res. Lett.* 32: L14613.
- Dmitrenko, I.A., Kirillov, S.A. & Tremblay, L.B. (2008): The long-term and interannual variability of summer fresh water storage over the eastern Siberian shelf: Implication for climatic change.- *J. Geophys. Res.* 113: C03007.
- Dmitrenko, I.A., Kirillov, S.A., Krumpfen, T., Makhotin, M., Abrahamsen, E.P., Willmes, S., Bloshkina, E., Hölemann, J., Kassens, H. & Wegner, C. (2010): Wind-driven diversion of summer river runoff preconditions the Laptev Sea coastal polynya hydrography: Evidence from summer-to-winter hydrographic records of 2007-2009.- *Continent. Shelf Res.* 30 (15): 1656-1664.
- Dmitrenko, I., Kirillov, S., Tremblay, L., Kassens, H., Anisimov, O., Lavrov, S., Razumov, S. & Grigoriev, M. (2011): Recent changes in shelf hydrography in the Siberian Arctic: Potential for subsea permafrost instability.- *J. Geophys. Res.* 116: C10027.
- ECMWF – *European Centre for Medium-Range Weather Forecasts*, <<http://apps.ecmwf.int/datasets/>> [last access: 15 May 2017].
- Eliseev, A., Malakhova, V., Arzhanov, M., Golubeva, E., Denisov, S. & Mokhov, I. (2015): Changes in the boundaries of the permafrost layer and the methane hydrate stability zone on the Eurasian Arctic Shelf, 1950-2100.- *Doklady Earth Sci.* 465(2): 1283-1288.
- Fofonova, V., Danilov, S., Androsov, A., Janout, M., Bauer, M., Overduin, P., Itkin, P. & Wiltshire K.H. (2015): Impact of wind and tides on the Lena River freshwater plume dynamics in the summer season.- *Ocean Dynamics* 65(7): 951-968.
- Golubeva, E.N., Ivanov, Ju.A., Kuzin, V.I. & Platov, G.A. (1992): Numerical modeling of the World Ocean circulation including upper ocean mixed layer.- *Oceanology, Engl. Transl.* 32(3): 395-405.
- Golubeva, E.N. & Platov, G.A. (2007): On improving the simulation of Atlantic Water circulation in the Arctic Ocean.- *J. Geophys. Res.* 112: C04S05.
- Golubeva, E.N. & Platov, G.A. (2009): Numerical Modeling of the Arctic Ocean Ice System Response to Variations in the Atmospheric Circulation from 1948 to 2007.- *Izvestiya, Atmospheric and Oceanic Physics* 45: 137-151.
- Guay, C.K., Falkner, R.D., Muench, R.D., Mensch, M., Frank, M. & Bayer, R. (2001): Wind-driven transport pathways for Eurasian Arctic river discharge.- *J. Geophys. Res.* 106: 11469-11480.
- Harms, I.H., Karcher, M.J. & Dethleff, D. (2000): Modelling Siberian river runoff – implications for contaminant transport in the Arctic Ocean.- *J. Mar. Systems* 27:95-115.
- Hölemann, J.A., Kirillov, S., Klagge, T., Novikhin, A., Kassens, H. & Timokhov, L. (2011): Near-bottom water warming in the Laptev Sea in response to atmospheric and sea-ice conditions in 2007.- *Polar Research* 30: 6425.
- Hunke, E.C. & Dukowicz, J.K. (1997): An elastic-viscous-plastic model for ice dynamics.- *J. Phys. Oceanogr.* 27(9): 1849-1867.
- Jakobsson, M., Mayer, L.A., Coakley, B., Dowdeswell, J.A., Forbes, S., Fridman, B., Hodnesdal, H., Noormets, R., Pedersen, R., Rebesco, M., Schenke, H.-W., Zarayskaya, Y.A., Accettella, D., Armstrong, A., Anderson, R.M., Bienhoff, P., Camerlenghi, A., Church, I., Edwards, M., Gardner, J.V., Hall, J.K., Hell, B., Hestvik, O.B., Kristoffersen, Y., Marcussen, C., Mohammad, R., Mosher, D., Nghiem, S. V., Pedrosa, M. T., Travaglini, P.G., & Weatherall, P. (2012): *The International Bathymetric Chart of the Arctic Ocean (IBCAO) Version 3.0*.- *Geophys. Res. Lett.* 39: L12609
- Janout, M.A., Hölemann, J. & Krumpfen, T. (2013): Cross-shelf transport of warm and saline water in response to sea ice drift on the Laptev Sea shelf.- *J. Geophys. Res. Oceans.* 118: 563-576.
- Janout, M., Hölemann, J., Juhls, B., Krumpfen, T., Rabe, B., Bauch, D., Wegner, C., Kassens, H. & Timokhov, L. (2016): Episodic warming of

- near-bottom waters under the Arctic sea ice on the central Laptev Sea shelf.- *Geophys. Res. Lett.* 43(1): 264-272.
- Johnson, M.A. & Polyakov, I. (2001): The Laptev Sea as a source for recent Arctic Ocean salinity change.- *Geophys. Res. Lett.* 28(10): 2017-2020.
- Kalnay, E., Kanamitsu, M., Kistler, R., Collins, W., Deaven, D., Gandin, L., Iredell, M., Saha, S., White, G., Woolen, J., Zhu, Y., Chelliah, M., Ebisuzaki, W., Higgins, W., Janowiak, J., Mo, K.C., Ropelewski, C., Wang, J., Leetma, A., Reynolds, R., Jenne, R. & Joseph, D. (1996): The NCEP/ NCAR 40-Year Reanalysis Project.- *Bull. Amer. Meteorol. Soc.* 77: 437-471.
- Kassens, H. & Karpiy, V. (1994): Russian German Cooperation: The Transdrift I Expedition to the Laptev Sea.- *Rep. Polar Res.* 151: 1-168.
- Kassens, H., Thiede, J., Bauch, H.A., Hölemann, J.A., Dmitrenko, I., Pivovarov, S., Priamnikov, S., Timikhov, L. & Wegner, C. (2007): The Laptev Sea system since the last glacial.- *Geol. Soc. Amer. Spec. Papers* 426: 89-96.
- Kulakov, M.U. (2008): Water circulation and transport of suspended sediments in the Laptev and East-Siberian seas.- *Arctic and Antarctic problems* 3(80): 86-97 (In Russian).
- Leonard, B.P. (1979): A stable and accurate convective modeling procedure based on quadratic upstream interpolation.- *Computer Methods Applied Mechanics & Engineering* 19: 59-98.
- Leonard, B.P., Lock, A.P. & MacVean, M.K. (1996): Conservative explicit unrestricted-timestep multidimensional constancy-preserving advection schemes.- *Mon. Weather Rev.* 124: 2588-2606.
- Lipscomb, W.H. & Hunke, E.C. (2004): Modeling Sea Ice Transport Using Incremental Remapping.- *Mon. Weather Rev.* 132(6):1341-1354.
- Malakhova, V.V. & Golubeva, E.N. (2014): Modeling of the dynamics subsea permafrost in the East Siberian Arctic Shelf under the past and the future climate change.- *Proc. SPIE. 20<sup>th</sup> Internat. Sympos. Atmospher. & Ocean Optics, Atmospheric Physics:* 9292: 92924D.
- Malakhova, V.V. (2015): Modeling of current state of the subsea permafrost of the East Siberian Shelf.- *Proc. Internat. Conf. "Geo-Siberia-2015". Novosibirsk:* SGGGA. 4(1): 155-159
- Malakhova, V.V. (2016): On the thermal influence of thermokarst lakes on the subsea permafrost evolution.- *Proc. SPIE 10035, 22<sup>nd</sup> Internat. Sympos. Atmospher. & Ocean Optics, Atmospheric Physics:* 100355: 100355U.
- Malakhova, V.V. & Eliseev, A.V. (2017): The role of heat transfer time scale in the evolution of the subsea permafrost and associated methane hydrates stability zone during glacial cycles. - *Global Planet. Change* 157: 18-25. *NCEP/NCAR Reanalysis 1* [last access: 15 November 2017]. <<http://www.esrl.noaa.gov/psd/data/reanalysis/reanalysis.shtml>>
- NCEP-DOE Reanalysis 2* [last access: 2 November 2017]. <<http://www.esrl.noaa.gov/psd/data/gridded/data.ncep.reanalysis2.html>>
- Nicolosky, D.J., Romanovsky, V.E., Romanovskii, N.N., Kholodov, A.L., Shakhova, N.E. & Semiletov, I. P. (2012): Modeling sub-sea permafrost in the East Siberian Arctic Shelf: The Laptev Sea region.- *J. Geophys. Res.* 117: F03028 .
- Overduin, P.P., Hubberten, H.-W., Rachold, V., Romanovskii, N., Grigoriev, M. & Kasymkaya, M. (2007): The evolution and degradation of coastal and offshore permafrost in the Laptev and East Siberian seas during the last climatic cycle.- *Geol. Soc. Amer. Spec. Papers* 426: 97-111.
- Pavlov, V.K. & Pavlov, P.V. (1999): Features of seasonal and interannual variability of the sea level and water circulation in the Laptev Sea.- In: H. KASSENS et al (ed), *Land-Ocean Systems in the Siberian Arctic – Dynamics and History*, Springer-Verlag, Berlin Heidelberg: 3-16.
- Platov, G. & Klimova, E. (2014): The results of numerical simulation of the Lena River runoff with the assimilation of satellite data: summer 2008.- *Bull. Novosibirsk Computing Center, Numerical Modeling in Atmosphere, Ocean and Environment Studies* 14: 55-72.
- Razumov, S.O., Spektor, V.B. & Grigoriev, M.N. (2014): A Model of the Late-Cenozoic Cryolithozone Evolution for the Western Laptev Sea Shelf.- *Okeanologiya* 54( 5): 679-693.
- Romanovskii, N.N., Hubberten, H.W., Gavrilov, A.V., Eliseeva, A.A. & Tipenko G.S. (2005): Offshore permafrost and gas hydrate stability zone on the shelf of East Siberian Seas.- *Geo Mar. Lett.* 25: 167-182.
- Shakhova, N., Semiletov, I., Leifer, I., Rekant, P., Salyuk, A. & Kosmach, D. (2010): Geochemical and geophysical evidence of methane release from the inner East Siberian Shelf.- *J. Geophys. Res.* 115: C08007.
- Shakhova, N., Semiletov, I., Leifer, I., Sergienko, V., Salyuk, A., Kosmach, D., Chernykh, D., Stubbs, Ch., Nicolsky, D., Tumskey, V. & Gustafsson, O. (2014): Ebullition and storm-induced methane release from the east Siberian Arctic shelf.- *Nature Geoscience* 7: 64-70.
- Shiklomanov, A.I. & Lammers, R.B. (2014): River ice responses to a warming Arctic - recent evidence from Russian rivers.- *Environ. Res. Lett.* 9: 035008.
- Shlychkov, V.A., Platov, G.A. & Krylova, A.I. (2014): A coupled hydrodynamic system of the Lena River delta and the Laptev Sea shelf zone: the model tuning and preliminary results of numerical simulation.- *Bull. Novosibirsk Computing Center, Numerical Modeling in Atmosphere, Ocean & Environment Studies* 14:81-103.
- Shpaikher, O., Fedorova, Z.P. & Yankina, Z.S. (1972): Interannual variability of hydrological regime of the Siberian shelf seas in response to atmospheric processes.- *Proc. AARI*, 306: 5-17 (in Russian).
- Steele, M. & Boyd, T. (1998): Retreat of the cold halocline layer in the Arctic Ocean.- *J. Geophys. Res.* 103 (C5): 10419-410435.
- Steele, M., Morley, R. & Ermold, W. (2000): PHC: A global hydrography with a high quality Arctic Ocean.- *J. Climate.* 14(9): 2079-2087. PHC-Polar Science Center Hydrographic Climatology [access: 2 April 2017] <[http://psc.apl.washington.edu/nonwp\\_projects/PHC/Climatology.html](http://psc.apl.washington.edu/nonwp_projects/PHC/Climatology.html)>
- Steele, M. & Ermold, W. (2004): Salinity trends on the Siberian shelves.- *Geophys. Res. Lett.* 31: L24308.
- Vörösmarty, C.J., Fekete, B.M & Tucker, B.A. (1998): *Global River Discharge, 1807-1991, Version. 1.1 (RivDIS)*. ORNL DAAC, Oak Ridge, Tennessee, <<https://doi.org/10.3334/ORNLDAAC/199>> [last access:15 November 2017.]
- Weingartner, T.J., Danielson, S., Sasaki, Y., Pavlov, V. & Kulakov, M. (1999): The Siberian coastal current: A wind- and buoyancy-forced Arctic coastal current.- *J. Geophys. Res.* 104: 29697-29714.
- Whitefield, J., Winsor, P., McClelland, J. & Menemenlis, D. (2015): A new river discharge and river temperature climatology data set for the pan-Arctic region.- *Ocean Modelling* 88: 1-15.
- Zakharov, V.F. (1966): The role of flaw leads off the edge of fast ice in the hydrological and ice regime of the Laptev Sea.- *Oceanology, Engl. Transl.* 6(1): 815-821.